SHORT THESIS FOR THE DEGREE OF DOCTOR OF PHILOSOPHY (PHD)

Myocardial sarcomere dysfunction

in acute and chronic rat models

by Árpád Kovács, MD

Supervisor: Judit Barta, MD, PhD

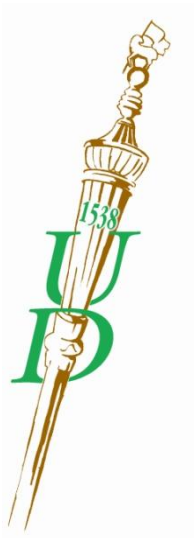

UNIVERSITY OF DEBRECEN

KÁLMÁN LAKI DOCTORAL SCHOOL

DEBRECEN, 2017

Myocardial sarcomere dysfunction in acute and chronic rat models

by Árpád Kovács, MD

Supervisor: Judit Barta, MD, PhD

Kálmán Laki Doctoral School, Universtiy of Debrecen

Head of the **Examination Committee:**	János Kappelmayer, MD, PhD, DSc
Members of the Examination Committee:	Albert Varga, MD, PhD, DSc
	Róbert Pórszász, MD, PhD

The examination takes place at the Library of Department of Laboratory Medicine, Faculty of Medicine, University of Debrecen, 09:00 21. February 2019.

Head of the **Defense Committee:**	János Kappelmayer, MD, PhD, DSc
Reviewers:	Csaba Csonka, MD, PhD
	Balázs Horváth, MD, PhD
Members of the Defense Committee:	Albert Varga, MD, PhD, DSc
	Róbert Pórszász, MD, PhD

The PhD Defense takes place at the Lecture Hall of Department of Cardiology, Faculty of Medicine, University of Debrecen, 11:00 21. February 2019.

1. INTRODUCTION AND BACKGROUND

1.1. Heart failure: a global public health challenge

In developed countries prevalence of heart failure is 1-2%, with 50% and 10% of 5- and 10-year mortality following diagnosis, respectively. Heart failure is a heterogeneous and complex syndrome that may result from any form of dysfunction in systolic or diastolic capacity. In elderly with cardiovascular co-morbidities (e.g. hypertension) heart failure often develops with preserved ejection fraction (≥50%, HFpEF). In acute coronary syndrome left ventricular myocardial infarction is the major cause of reduced ejection fraction (<40%, HFrEF). However, prevalence and mortality of all heart failure phenotypes are high.

The cardiac sarcomere is the smallest functional unit of the heart. Pathophysiological modulation of structural, functional and regulatory proteins of the sarcomere thereby interferes with the fine tuning of contraction-relaxation cycles of cardiomyocytes. During cardiac remodelling acute degradation or chronic dysregulation of myofilament proteins contribute to sarcomere dysfunction, leading to impaired cardiomyocyte force generating capacity and elasticity in the failing heart.

Revascularization is the primary therapy in myocardial infarction. At the same time, ischemia-reperfusion injuries are associated with the intervention, and big challenges in human. It is also known that hypertension is the most common co-morbidity of heart failure, in which the pathological activity of the renin-angiotensin system (RAS) plays a central role. However, the clinical effectiveness of RAS inhibitors in treating HFpEF is controversial, in striking contrast with their beneficial effects in HFrEF.

1.2. Physiological bases of sarcomere function

Cardiomyocyte mechanical work is determined by the interplay of contractile (active) and non-contractile elastic and viscous (passive) elements of the sarcomere.

Mechanism of myocardial contraction is based on forming and breaking cross-bridges between actin molecules and ’heads’ of myosin molecules. As a result of the cross-bridge cycle sliding of interdigitating thin (actin) and thick (myosin) filaments brings the Z discs closer together, therefore the sarcomere shortens. This mechanism is known as the ’sliding filament theory’.

During diastole intracellular [Ca^{2+}] is low, and the regulatory troponin complex [cardiac troponin C (cTnC), I (cTnI), T (cTnT)] and tropomyosin inhibit the force generating actin-myosin interaction. During systole the rise of intracellular [Ca^{2+}] induces and maintains the myofilament sliding. Chemical energy required for myofilament contraction originates from adenosine triphosphate (ATP) hydrolysis through myosin ATPase. ATP binding again to myosin heads is needed for cardiac muscle relaxation, otherwise the actin-myosin complex stiffens (rigor). Thus, the myosin motor molecule generates force and motion by co-ordinating its ATPase activity with its cyclic interaction with actin.

Myosin is formed by two of myosin heavy chain (MHC), two of essential myosin light chain (MLC-1), and two of regulatory myosin light chain (MLC-2). MHC isoform composition is correlated with the rate and energetics of force generation. In mammalians α-MHC and β-MHC are known and encoded by two distinct MHC genes. Rodent ventricular myocardium contains mainly α-MHC (~90%), while human ventricular myocardium contains predominantly β-MHC isoform.

The major determinant of cardiomyocyte passive tension, the merit of cellular diastolic function, is the giant protein titin. With a molecular mass ranging from 3,000 to 3,700 kDa, titin is the largest known polypeptide and its function as a molecular spring is responsible for the passive elasticity of muscle. Spanning the half sarcomere from the Z-disk to the M-band, titin is expressed in varying isoforms that confer differing elastic properties. Two main isoforms of titin are expressed in the human heart: a shorter, stiffer N2B (3,000 kDa) isoform

and a longer, more compliant N2BA isoform (>3,200 kDa). The elastic region of titin is located in the I-band of the sarcomere, in which the 'PEVK' segment (rich in proline, glutamate, valine, and lysine) is one of the intrinsically disordered structures. The composition of titin isoforms differs among species, with N2B predominating in rodents and N2BA in larger mammals. Long titin isoforms (N2BA) give rise to low passive stiffness, while short isoforms (N2B) ensure high passive stiffness.

In chronic cardiovascular disease (e.g. HFpEF) phosphorylation changes of titin by a variety of kinases result in different effects on the passive mechanical properties of the sarcomere. Protein kinase Cα (PKCα) has been shown to phosphorylate titin exclusively at the PEVK region (e.g. at Ser-12742 and Ser-12884 in the rat, and Ser-11878 and Ser-12022 in the human sequence) and to result in increased stiffness and viscosity.

Under pathological conditions shift in isoform composition, changes in oxidative and phosphorylation statuses, and degradation of myofilaments (actin, myosin and titin) and regulatory proteins (troponin complex and tropomyosin) may directly influence on one hand the performance, Ca^{2+}-sensitivity and kinetics of force generation, on the other hand the titin-dependent passive tension.

1.3. Role of Ca^{2+} in acute myocardial dysfunction: the Ca^{2+} paradox phenomenon

Acute myocardial injury due to coronary occlusion is a process with two faces. One obvious pathological factor is the ischemia itself, but the other one is the reperfusion in certain cases (ischemia/reperfusion injury). Current first-line therapy of acute myocardial infarction is early coronary revascularization, that limits infarct size, preserves left ventricular systolic function, and retards chronic remodelling and heart failure. However, paradoxically reperfusion may contribute to myocardial injury during infarct.

When a physiologically perfused isolated heart is perfused for a short period of time with a Ca^{2+} free, otherwise normal Krebs-Henseleit buffer, then with buffer ensuring again

physiological [Ca^{2+}], the heart rapidly deteriorates. This adverse effect of Ca^{2+} repletion on a once Ca^{2+} depleted heart is known as Ca^{2+} paradox. Although *in vivo* pathophysiology does not present exclusive depletion and repletion of Ca^{2+} during ischemia and reperfusion, extreme rise of cytosolic [Ca^{2+}] is a key element of ischemia/reperfusion injury. For that very reason an isolated heart undergoing Ca^{2+} paradox has been considered to serve a widely accepted model for investigating the mechanisms of structural and functional myocardial injury due to intracellular Ca^{2+} overload as part of ischemia/reperfusion injury.

The consequence of Ca^{2+} repletion after Ca^{2+} depletion on global left ventricular function is a marked decrease in systolic pressure paralleled by a significant increase in end-diastolic pressure. The rationale of dramatic contractile impairment due to Ca^{2+} paradox is myocardial hypercontracture associated with intense ultrastructural damage.

Accordingly, Ca^{2+} depletion initiates a moderate disruption of the adjacent cardiac cells at the intercalated discs, then cell-to-cell and cell-extracellular matrix connections break up. Finally, in massive Ca^{2+} overload hypercontracture develops, while the heart becomes pale because of myoglobin loss.

At the same time, numerous intracellular changes occur in the isolated heart exposed to Ca^{2+} paradox, collectively provoking intracellular Ca^{2+} overload, therefore leading to extensive perturbations of intracellular Ca^{2+} handling. However, it has not been elucidated yet whether sarcomere disruption and myofilament damage also contribute to the contractile failure in Ca^{2+} paradox. In rat models of Ca^{2+} paradox MLC-1 release and troponin I release together with α-fodrin degradation have been reported. Despite Ca^{2+} paradox has not been a hot topic lately, recent scientific efforts apparently still have been able to provide new insights into the mechanism of Ca^{2+} overload induced changes.

1.4. Pathophysiological role of the RAS in chronic myocardial dysfunction

The enzymatic cascade of RAS is a key element in regulating blood pressure, therefore alterations of RAS are crucial in inducing and maintaining hypertension. Hypertension is the most common human disease and the most prevalent co-morbidity of heart failure. Typically in the HFpEF phenotype associated with hypertension, hypertrophy and fibrosis of the left ventricle stiffen the myocardium, subsequently impair left ventricular relaxation and diastolic filling, and diastolic dysfunction develops in the end.

In cardiovascular disease the pathological effects of angiotensin II are mediated by acting on the type AT_1R receptor, that include increased sympathetic tone and aldosterone secretion, vasoconstriction, retention of salt and water, immune and inflammatory responses, and global cardiovascular cell proliferation and remodelling. In contrast, the ACE homologous ACE2 enzyme is a counter-regulatory element in RAS signalling. ACE2 is responsible for angiotensin II breakdown, producing angiotensin 1-7 molecule, that mediates beneficial effects by acting on the Mas receptor (MasR), such as vasodilation, natriuresis, tissue healing, differentiation, apoptosis and limited cell proliferation. Findings therefore suggest the existence of two axis with opposing effects in RAS signalling, namely the classical ACE – angiotensin II – AT_1R axis and the alternative ACE2 – angiotensin 1-7 – MasR axis. Interestingly, taking into consideration that angiotensin I and II are substrates of ACE2, the activity of the alternative pathway depends on the amount of these peptides from the classical pathway. ACE2 is the negative regulator of the angiotensin II-induced myocardial hypertrophy, fibrosis and diastolic dysfunction, thus lack of ACE2 in hypertension and myocardial infarction leads to adverse pathological remodelling.

Effectiveness of RAS inhibitors confirms the central role of RAS in the pathophysiology of hypertension, thereby in the development of heart failure. Nonetheless, heart failure implies distinct entities, since the pathomechanism and therapy of HFpEF is

being different from that of HFrEF in human. Interestingly, the clinical effectiveness of RAS inhibitors is controversial, since these drugs work in HFrEF, but fail in HFpEF. HFpEF in fact still lacks proven therapy.

This contradictory clinical practice supports the relevance of investigating the renin overexpression transgenic rat (mRen2) model of hypertension. Pathophysiological role of tissue angiotensin II has been revealed in these animals, the mRen2 model is therefore suitable to study myocardial dysfunction related to the local pathological RAS signalling. Noteworthy is that the features of the mRen2 phenotype are similar to those observed in human heart failure. The mRen2 myocardium exhibits hypertrophy, extracellular collagen accumulation and perivascular fibrosis, as well as angiotensin II-mediated oxidative stress. In addition, some *in vivo* studies found decreased left ventricular systolic function (ejection fraction), reduced positive inotropic response of papillary muscles to isoproterenol with decreased Ca^{2+}-sensitivity of skinned fibers in these animals. These functional traits are characteristic for systolic dysfunction and the HFrEF phenotype. In contrast, other *in vivo* reports suggested normal ejection fraction, but diastolic dysfunction in the mRen2 strain. Impaired myocardial relaxation of mRen2 rats may be attributable to increased diastolic tension of skinned left ventricular fibers from these hearts. In summary, it appears that myocardial dysfunction of hypertensive mRen2 rats appropriately reflects the diversity of cardiac remodelling in human.

2. AIMS

2.1. Investigation of the mechanism of sarcomere dysfunction in Ca^{2+} paradox

We aimed to explore the potential functional and structural sarcomere dysfunction in the background of depressed global contractility of the heart after Ca^{2+} overload. In our work on rat hearts exposed to Ca^{2+} paradox we tested Ca^{2+}-stimulated and Mg^{2+} ATPase activities of ventricular myofibrils, contractile performance of single cardiomyocytes, and whether or not molecular targets such as contractile (e.g. actin, myosin), structural (e.g. titin, α-actinin) and regulatory (e.g. troponin complex, MLC) myofilament proteins are injured.

2.2. Investigation of the role of local RAS in diastolic dysfunction

The purpose of our study was to determine how pathological activation of the RAS affects myocardial sarcomere function in the renin overexpressing mRen2 rat strain. In our work on 15-week-old male homozygous mRen2 rats we studied the myocardial RAS (ACE and ACE2 activities), the mechanical performance of isolated cardiomyocytes, the PKCα expression on the angiotensin II pathway, and the phosphorylation of titin that is responsible for passive tension of the sarcomere.

3. MATERIALS AND METHODS

3.1. Methods I: the Ca^{2+} paradox model

3.1.1. Ethical approvals and animal care

Experimental protocols were approved by the University of Manitoba Animal Care Committee and follow the guidelines of the Canadian Council on Animal Care and the guidelines of the National Institute of Health.

3.1.2. Ca^{2+} paradox by Langendorff

Male Sprague-Dawley (SD, 250-300 g) rat hearts were perfused with Krebs-Henseleit solution (120.0 mM NaCl, 4.8 mM KCl, 1.2 mM KH_2PO_4, 1.25 mM $CaCl_2$, 1.25 mM $MgSO_4$, 25.0 mM $NaHCO_3$ and 8.6 mM glucose; pH 7.4) by using Langendorff method (37 °C, 95% O_2, 5% CO_2). Hearts were electrically stimulated (300 stimuli/min). Following a 20 min stabilization, hearts were randomized into three groups (n = 7-9/groups). Hearts were exposed either to normal Krebs-Henseleit buffer containing 1.25 mM Ca^{2+} for 15 min (control), or to Ca^{2+} depletion for 5 min (Ca^{2+} depletion), or to Ca^{2+} repletion with normal Krebs-Henseleit buffer for 10 min after 5 min of Ca^{2+} depletion (Ca^{2+} paradox). Water-filled latex balloon was placed into the left ventricular cavity and connected to a transducer. Left ventricular developed pressure and end-diastolic pressure were registered, and rates of pressure development (dP/dt_{max}) and pressure decay (dP/dt_{min}) were determined.

3.1.3. Myofibrillar ATPase activity

Left ventricular myofibrils were isolated (n = 7-9/groups) and suspended in a suspension medium (100.0 mM KCl, 20.0 mM Tris_HCl; pH 7.0). Total ATPase activity was measured in the following buffer: 20.0 mM imidazole, 3.0 mM $MgCl_2$, 2.0 mM Na_2ATP, 5.0 mM NaN_3, 50.0 mM KCl, 0.01 mM free Ca^{2+}; pH 7.0. Mg^{2+} ATPase activity was determined in the same buffer, except free Ca^{2+} was replaced by 1.0 mM EGTA. Reactions were run for 5 min at 37 °C, then terminated by adding ice-cold 12% trichloroacetic acid. Following centrifugation, phosphate was determined in the supernatant by colorimetric method. Ca^{2+}-stimulated ATPase activity was calculated from the total and basal (Mg^{2+}) ATPase activity.

Experimental setup for contractile force measurements of isolated cardiomyocytes

Deep-frozen (–70 °C) tissue samples from Langendorff-perfused hearts (n = 5-7/group) were mechanically disrupted and membrane-permeabilized by 0.5% Triton X-100 detergent in

isolating solution (1.0 mM $MgCl_2$, 100.0 mM KCl, 2.0 mM EGTA, 4.0 mM ATP, 10.0 mM imidazole; pH 7.0) at 4 °C. Each subjected cell was attached to a length controller and a force transducer at 15 °C. Cardiomyocyte isometric force generation was recorded at sarcomere length of 2.3 μm (n = 12-13/group). Ca^{2+}-dependent force production of a single cardiomyocyte was induced by transferring the preparation from relaxing (10.0 mM BES, 37.11 mM KCl, 6.41 mM $MgCl_2$, 7.0 mM EGTA, 6.94 mM ATP, 15.0 mM creatine-phosphate; pH 7.2) to activating solution (same composition as relaxing solution aside from containing CaEGTA instead of EGTA). In our experiments Ca^{2+} concentrations were indicated as $-\log_{10}[Ca^{2+}]$ units. Protease inhibitors were added to all solutions freshly: phenylmethylsulfonyl fluoride (PMSF): 0.5 mM; leupeptin: 40 μM; and E-64: 10 μM. Maximal and submaximal Ca^{2+}-activated force generation of isolated cardiomyocytes was registered by using maximal activating solution (pCa 4.75) and submaximal activating solutions (pCa 5.4-7.0). Rate constant of force redevelopment (k_{tr}) and Ca^{2+}-sensitivity of the contractile machinery (pCa_{50}) were determined. Ca^{2+}-independent passive force of subjected cardiomyocytes was measured in relaxing solution (pCa 9.0).

Polyacrylamide gel electrophoresis (PAGE)

Left ventricular myocardial tissue samples (n = 5/group) were pulverized in a chilled mortar and homogenized in an ice-cold buffer containing 30.0 mM KCl, 15.0 mM imidazole, 5.0 mM NaCl, 1.0 mM $MgCl_2$, 1.0 mM EGTA, 1.0 mM EDTA, 0.5 mM DTT and $CaCl_2$, 0.3 mM Calpain Inhibitor I, leupeptin and Phosphatase Inhibitor Cocktail 1; pH 7.5. Homogenates were boiled in sodium dodecyl sulfate (SDS) sample buffer for 3 min. One-dimensional SDS-PAGE was performed in a non-stacking gradient gel system (concentration range: 6-18%) followed by silver staining. Suspected small myofilament proteins (about ≤100 kDa) were separated on single-concentration SDS-polyacrylamide gels (α-actinin: 7%; desmin: 10%; actin, cTnT, Tm and cTnI: 15%; MLC-1 and MLC-2: 20%).

Western immunoblot

Myofilament proteins were identified by Western immunoblot, where membranes were probed with the following primary antibodies: anti-α-actinin clone EA-53 (Sigma-Aldrich), dilution 1:5,000; anti-desmin clone DE-U-10 (Sigma-Aldrich), dilution 1:7,000; anti-actin (Abcam), dilution 1:1,000; anti-cTnT clone 1A11 (Research Diagnostics), dilution 1:3,000; anti-Tm (Sigma-Aldrich), dilution 1:600; anti-cTnI clone 19C7 (Research Diagnostics), dilution 1:1,000; anti-MLC-1 (Santa Cruz Biotechnology), dilution 1:7,000; anti-MLC-2 (Abcam), dilution 1:400.

MHC isoform analysis

Ventricular tissues (n = 5/group) were homogenized under denaturing conditions. MHC isoforms (α and β) were separated on a 4% polyacrylamide gel at a constant 220 V for 3-3.5 h at around 15 °C. Gels were stained with Coomassie blue. Human failing heart ventricular sample served as α-MHC and β-MHC isoform control. For MHC Western immunoblot analysis cardiac tissues (n = 4-6/group) were prepared as for the mechanical measurements, except that the isolated samples were dissolved in sample buffer instead of isolating solution. Male Sprague-Dawley soleus muscle was used as β-MHC control. After transfer membranes were probed with the following primary antibodies: pan anti-MHC (Sigma-Aldrich), dilution 1:10,000; and anti-β-MHC isoform: mouse IgM, MYH7 (A4.840) sc-53089 (Santa Cruz Biotechnology), dilution 1:1,000.

Titin assays

Ventricular tissue samples (n = 3 in duplicates/group) were prepared as for the mechanical measurements, and dissolved in SDS sample buffer [urea: 8.0 M; thiourea: 2.0 M; SDS: 3.0%; dithiothreitol (DTT): 75.0 mM; Tris_HCl (pH 6.8): 0.05 M; glycerol: 10.0%; brome-phenol blue: 0.004%; leupeptin: 40.0 μM; E-64: 10.0 μM]. Human failing heart

ventricular sample served as N2BA and N2B titin isoform control. PAGE was performed by using 2% agarose-strengthened gel to separate titin. Gels were run at 2 mA constant current for 540 min. Gels were stained with Coomassie brilliant blue.

Statistical analysis

Data are expressed as mean ± SEM. Differences between groups were evaluated by one-way ANOVA followed by Bonferroni *post-hoc* test, where P values of <0.05 were considered statistically significant.

3.2. Methods II: the mRen2 model

Ethical approvals and animal care

All animal care and experimental procedures were approved by the Ethical Committee of the University of Debrecen (Ethical Statement number: 1/2013/DE MÁB) and conformed to Directive 2010/63/EU of the European Parliament. Transgenic mRen2 rats were compared to SD rats (n = 6) as geno- and phenotype controls.

Transgenic mRen2 rat model of hypertension

Male homozygous rats carrying the mouse *Ren-2*^{d} renin gene (mRen2, n = 6) were obtained from the *Max Delbrück Centrum Für Molekulare Medizin* (Berlin-Buch, Germany). Hearts of 15-week-old animals were excised, then left ventricle was further dissected in isolating solution, snap frozen in liquid nitrogen, and stored at –70 °C.

Myocardial ACE and ACE2 activities

About 0.1 g of deep frozen left ventricular samples (n = 4 from both SD and mRen2 rats) were homogenized in 10 volume of ice-cold Dulbecco's phosphate-buffered saline (DPBS, Ca^{2+} and Mg^{2+} free, Gibco). The reaction mixture for the measurement of ACE activity contained 6 µl heart homogenate in buffer (100.0 mM Tris_HCl, 15.0 µM Abz-FRK(Dnp)P, 50.0 mM NaCl, 10.0 µM $ZnCl_2$; pH 7.0). The reaction time was 45 min and

fluorescence intensities (excitation: 320 nm; emission: 405 nm) were measured at 60 s intervals. The measured values were plotted as the function of time and fitted by a linear regression. ACE activity was calculated by the equation: ACE activity = (S/k)*D/P; where S is the rate of increase in fluorescence intensity (slope), k is the increase in fluorescence intensity when 1 μmole of the substrate is being cleaved, D is the dilution factor (35 in these experiments) and P is the protein concentration (in mg/ml). 1 unit (U) represents 1 μmole substrate cleavage in 1 min by 1 mg of protein.

For the measurement of ACE2 activity 20 μl of tissue homogenate was added to the reaction mixture containing protease inhibitors: 10.0 μM Bestatin-hidrochloride; 10.0 μM Z-prolyl-prolinal; 5.0 μM Amastatin-hidrochloride; 10.0 μM Captopril and 5.0 mM NaCl; 100.0 μM $ZnCl_2$; 75.0 mM Tris_HCl; pH 6.5. Reaction temperature was 37 °C. Fluorescence intensities (excitation: 320 nm; emission: 405 nm) were measured in 6 min intervals for 84 min. Values were plotted as a function of time and fitted by a linear regression. Fit was accepted when r^2 >0.8. ACE2 activity was calculated according to the equation: ACE2 activity = (S/k)*D/P; where S is the rate of increase in fluorescence intensity (slope), k is the increase in fluorescence intensity when 1 nmole of the substrate is being cleaved and D is the dilution factor (10 in these experiments), P is the protein concentration (in mg/ml). 1 unit (U) represents 1 nmole substrate cleavage in 1 min by 1 mg of protein.

Force measurements on isolated cardiomyocytes

Mechanical performance of isolated cardiomyocytes (n = 5-6/heart) from SD control and mRen2 hearts (n = 4/group) were tested according to the protocol in Ca^{2+} paradox.

Titin assays

Separation and identification of titin in SD and mRen2 left ventricular tissue samples (n = 4 duplicates/group) were carried out as for Ca^{2+} paradox. Gels containing SD and mRen2 samples were also stained for 90 min with Pro-Q Diamond phospho-protein gel stain. Beyond

that, Western immunoblotting was applied to assess titin phosphorylation at particular serine residues of PEVK segment. Phospho-specific antibodies were developed against either Ser-11878 and Ser-12742 (PS26, GL Biochem, dilution 1:1,000) or Ser-12022 and Ser-12884 (PS170, Genscript, Piscataway, dilution 1:1,000) in the full human and rat titin sequence, respectively.

Protein kinase Cα (PKCα) and actin control Western immunoblot

About 0.1 g of deep frozen left ventricular heart samples (n = 4/group) were homogenized in 10-fold diluted ice cold DPBS (Ca^{2+} and Mg^{2+} free, Gibco). Homogenized samples were supplemented by equal volume of 2-fold concentrated SDS sample buffer and incubated for 10 min at 100 °C. PKCα expression was tested by anti-PKCα (Sigma-Aldrich, dilution 1:20,000) and anti-phospho(Ser-657/Tyr-658)-PKCα (EMD Millipore, dilution 1:500) antibodies. Actin expression was tested by an anti-actin antibody (Sigma-Aldrich, dilution 1:3,500).

Statistical analysis

Data are expressed as mean ± SEM. Differences between groups were evaluated by unpaired Mann-Whitney nonparametric test, where P values of <0.05 were considered statistically significant.

4. RESULTS

4.1. Contractile and myofibrillar dysfunction in Ca^{2+} paradox

Ca^{2+} paradox dramatically impairs left ventricle function

LVDP recorded in control hearts (127.4 ± 6.1 mmHg) was permanently decreased during both Ca^{2+} depletion (9.8 ± 1.3 mmHg, P<0.001) and Ca^{2+} paradox (12.9 ± 1.3 mmHg, P<0.001). Similarly, dP/dt_{max} and dP/dt_{min} in Ca^{2+} depletion (62.6 ± 6.9 and –87.9 ± 12.6 mmHg/sec, respectively, P<0.001), as well as in Ca^{2+} paradox (93.9 ± 19.7 and

–163.4 ± 17.9 mmHg/sec, respectively, P<0.001) were significantly lower than those in controls (7073.8 ± 351.0 and -4075.3 ± 206.2 mmHg/sec, respectively). At the same time, LVEDP of control hearts (4.1 ± 0.5 mmHg) was markedly increased due to both Ca^{2+} depletion (32.2 ± 3.3 mmHg, P<0.001) and Ca^{2+} paradox (72.4 ± 5.0 mmHg, P<0.001).

Myofibrillar Ca^{2+}-stimulated ATPase activity is decreased, while Mg^{2+} ATPase activity is increased in Ca^{2+} paradox

Compared to control hearts (12.08 ± 0.57 μmol P_i/mg protein/h), myofibrillar Ca^{2+}-stimulated ATPase activity was decreased upon Ca^{2+} depletion (8.13 ± 0.19 μmol P_i/mg protein/h, P<0.001), and it remained low in Ca^{2+} paradox (8.40 ± 0.22 μmol P_i/mg protein/h, P<0.001). In contrast, control Mg^{2+} ATPase activity (3.20 ± 0.25 μmol P_i/mg protein/h) was not altered by Ca^{2+} depletion (3.27 ± 0.10 μmol P_i/mg protein/h), but it was increased through Ca^{2+} paradox (7.21 ± 0.36 μmol P_i/mg protein/h, P<0.001).

Ca^{2+} paradox impairs Ca^{2+}-activated force generation of isolated cardiomyocytes

Maximal active tension of the Ca^{2+} depletion group was not significantly different (21.04 ± 2.32 kN/m^2) from the control values (25.07 ± 3.51 kN/m^2), but in the Ca^{2+} paradox group it was significantly lower (12.12 ± 3.19 kN/m^2, P<0.05). Relative to control k_{tr} at saturating Ca^{2+} levels ($k_{tr,max}$, 4.61 ± 0.22), myocytes from the Ca^{2+} depleted hearts had lower $k_{tr,max}$ (3.85 ± 0.21, P<0.05), such as those from Ca^{2+} paradoxical hearts (3.21 ± 0.23, P<0.001). Ca^{2+}-sensitivity (pCa_{50}) was 5.99 ± 0.02 in the Ca^{2+} depletion group, which was not significantly different from the pCa_{50} of the controls (5.94 ± 0.02). However, pCa_{50} was 5.90 ± 0.03 after Ca^{2+} repletion, indicating lower Ca^{2+}-sensitivity than that in Ca^{2+} depletion (P<0.05). Relative to control (2.13 ± 0.29 kN/m^2), no change was observed in passive tension neither upon Ca^{2+} depletion (2.11 ± 0.54 kN/m^2) nor upon Ca^{2+} paradox (2.25 ± 0.35 kN/m^2).

4.2. α-MHC and cTnT degradation in Ca^{2+} paradox

Ca^{2+} paradox disturbs myofibrillar integrity: α-MHC and cTnT on target

Pan MHC Western immunoblot identified additional bands with higher mobility than the parent molecules in Ca^{2+} depletion and Ca^{2+} paradox groups, suggesting MHC degradation. β-MHC isoform was not recognized by Western immunoblot in our rat hearts. Therefore, the MHC we see is α-MHC, since only that isoform was expressed in our samples. The specific electrophoretic separation of MHC isoforms followed by Coomassie staining also confirms that the control samples express only the α-MHC isoform and this latter isoform showed up as a somewhat lower band in the Ca^{2+} depletion and Ca^{2+} paradox groups compared to the parent molecule of the controls, indicating protein degradation. Moreover, cTnT also exhibited a progressive degradation during Ca^{2+} depletion then Ca^{2+} repletion. We found no changes in α-actinin, desmin, actin, Tm, cTnI, MLC-1 and MLC-2 between the experimental groups. Titin did not show degradation in Ca^{2+} depletion and Ca^{2+} paradox.

4.3. Increased cardiomyocyte passive tension in mRen2 rats

Unaffected Ca^{2+}-activated force generation and increased Ca^{2+}-independent (passive) tension in mRen2 hearts

Ca^{2+}-activated maximal force generation was similar in mRen2 and SD rats (25.89 ± 0.99 and 29.05 ± 2.80 kN/m^2, respectively). Ca^{2+}-sensitivity of force production was also similar (5.83 ± 0.01 in mRen2 and 5.87 ± 0.05 in SD rats). In contrast, cardiomyocyte Ca^{2+}-independent tension was increased in the left ventricle of mRen2 rats (1.74 ± 0.06 kN/m^2), when compared to age-matched SD rats (1.28 ± 0.18 kN/m^2, $P<0.05$).

4.4. Correlation between the dysregulation of tissue RAS and the altered phosphorylation pattern of cardiac titin in the mRen2 model

Downregulation of the alternative RAS pathway in the mRen2 left ventricle

Left ventricular ACE activity was similar in both mRen2 and SD rats (0.26 ± 0.02 U/mg in mRen2 vs. 0.22 ± 0.02 U/mg in SD). In contrast, left ventricular ACE2 activity was lower in mRen2 rats when compared to SD rats (2.49 ± 0.40 U/mg vs. 3.82 ± 0.31 U/mg in SD, $P<0.05$).

Increased PKCα expression in mRen2 hearts

PKCα expression was increased by 1.78 ± 0.14-fold in mRen2 rats when compared to SD (1.00 ± 0.12, $P<0.01$). No difference in the level of phosphorylated (Ser-657/Tyr-658) PKCα was found when normalized to actin expression (1.25 ± 0.17 in mRen2 vs. 1.00 ± 0.06 in SD), nor when normalized to PKCα expression (0.79 ± 0.13 in mRen2 vs. 1.00 ± 0.10 in SD).

Hyperphosphorylation of titin PEVK element in the mRen2 animals

Protein gel staining and blot staining showed similar titin expression pattern in mRen2 and SD hearts. The major band representing the N2B isoform of titin was detected at about 3,000 kDa of molecular weight. Pro-Q Diamond showed similar levels of phosphorylation in mRen2 hearts when normalized to SD hearts (0.92 ± 0.04 vs. 1.00 ± 0.04, respectively). Similarly, no difference was found in the normalized phosphorylation level at Ser-12884 (0.92 ± 0.14 vs. 1.00 ± 0.08 in SD) within the PEVK element of titin. In contrast, mRen2 myocardium exhibited hyperphosphorylation at Ser-12742 (1.33 ± 0.12 vs. 1.00 ± 0.06 in SD, $P<0.05$) in the same (PEVK) region.

5. DISCUSSION

5.1. Degradation of contractile proteins leads to dysfunction of the actomyosin mechanoenzyme in experimental Ca^{2+} paradox

Our study aimed to investigate for the first time the influence of Ca^{2+} paradox on cardiac function at the myofibrillar level. Here we demonstrate that global contractile impairment of isolated hearts due to Ca^{2+} depletion then Ca^{2+} repletion is associated with altered myofibrillar ATPase activity and decreased Ca^{2+}-dependent cardiomyocyte force production. Furthermore, degradation of contractile proteins (α-MHC and cTnT) occurs in hearts affected by Ca^{2+}-paradox. These data suggest an insufficient actin-myosin interaction in intracellular Ca^{2+}-overload, leading to contractile dysfunction presumably on the basis of myofibrillar damage.

In accordance with prior findings in Ca^{2+} paradox we observed a dramatic decrease of left ventricular developed pressure and dP/dt_{max} in both Ca^{2+} depletion and Ca^{2+} paradox, indicating depressed global left ventricular systolic dysfunction. At the same time, as a result of the significant rise in left ventricular end-diastolic pressure and low dP/dt_{min} during Ca^{2+} depletion then Ca^{2+} replacement, these hearts manifested diastolic dysfunction as well, that is in line with increased myocardial resting tension.

In myofibrils from isolated hearts suffered Ca^{2+}-paradox here we documented an increased Mg^{2+}-dependent ATPase, but a decreased Ca^{2+}-stimulated ATPase activity. This observation implies that in Ca^{2+} paradox a higher rate of basal ATP hydrolysis on myosin heads is followed by a lower dissociation rate of ATP metabolites, contributing to stiffer actin-myosin interaction and/or local ATP consumption under relaxed conditions. In the regulation of cardiac contraction it is generally accepted that Mg^{2+}-ADP binds strongly to myosin, promoting the isometric tension and decreasing tension kinetics.

Experiments on rat skinned fibers have demonstrated that Mg^{2+}-ADP has a clear impact on rigor tension development as well as on myosin ATPase activity, suggesting that development of rigor cross-bridges might be related to an increase in myosin ATPase activity. Indeed, in rat permeabilized cardiomyocytes rigor was associated with enhanced myosin ATPase activity, in addition, Mg^{2+}-ADP was shown to stimulate myosin ATPase. These results propose an inhibitory effect of Mg^{2+}-ADP on dissociation steps and/or on further Mg^{2+}-ATP binding and cross-bridge detachment. It appears that the stimulated myosin ATPase in Ca^{2+}-paradox is the Mg^{2+}-dependent one, resulting in higher rate of ATP hydrolysis along with slower rate of P_i and ADP release. This apparent discrepancy may lead to a proportionally increased number of myosin heads bounded to actin in each cross-bridge cycle. The stiff actin-myosin interaction and/or elevated basal ATP consumption then may result in high resting tension. This theory may explain increased left ventricular end-diastolic pressure seen in Ca^{2+} paradox. On the other hand, we found that in Ca^{2+} depleted and Ca^{2+} paradoxical hearts, global impairment of systolic function was associated with depressed myofibrillar Ca^{2+}-stimulated ATPase activity. It has been known for a long time that myosin ATPase determines the velocity of muscle contraction, thus indices of Ca^{2+}-activated contraction rate (e.g. dP/dt) are tightly correlated with Ca^{2+}-stimulated ATPase activity of myofibrils as elementary for initiating power stroke. Consequently, low Ca^{2+}-stimulated ATPase activity is associated with reduced Ca^{2+}-dependent contraction, resulting in systolic dysfunction, like in Ca^{2+} paradoxical hearts.

Beyond that, for the first time we made an attempt to test cellular mechanical function in Ca^{2+} paradox, and described a significant decrease in maximal active tension and $k_{tr,max}$ of still surviving isolated cardiomyocytes after Langendorff-perfusion. These results from single cell preparations are consistent with our left ventricle contractility findings, since we consider reduced active tension as the cellular basis of depressed left ventricular developed pressure.

Drop in dP/dt_{max} is likely the global reflection of reduced $k_{tr,max}$ by reason of depressed Ca^{2+}-stimulated ATPase activity. In contrast to Ca^{2+}-dependent parameters, passive tension of isolated cardiomyocytes was not affected at all during Ca^{2+} depletion then Ca^{2+} replacement. Thus, passive myofilament components of diastole appear unlikely to be primarily responsible for myocardial stiffening in Ca^{2+} paradox.

In our biochemical assays we detected a gradual damage of α-MHC and cTnT en route to Ca^{2+} paradox. Based on previous observations, limited degradation of myofibrils may occur after Ca^{2+} paradox, suggesting cTnT release through membrane destruction. Likewise, homogenates from guinea pig hearts exposed to Ca^{2+} overload exhibited degradation of cTnT. A potential cross-linking between troponin subunits or their fragments and other cardiac proteins was therefore suggested in cell death after Ca^{2+} paradox. These results are clearly in accordance with our findings based on Western blot assays suggesting progressive cTnT degradation upon Ca^{2+} depletion and Ca^{2+} repletion, although we did not observe cross-linked cTnT forms.

5.2. Downregulation of local RAS is associated with increased cardiac titin-dependent passive tension in mRen2 rats

In our work we found a decrease in cardiac ACE2 activity that is normally responsible for angiotensin II breakdown, in addition to unaltered ACE activities in the mRen2 rats. Our findings suggest that cardiac elimination of angiotensin II is reduced in mRen2 animals, which potentially increases local RAS activity. Furthermore, in the left ventricle of mRen2 rats we found an increase in the expression level of cardiac PKCα as part of the intracellular angiotensin II pathway. Hyperphosphorylation at the PEVK element of titin the molecule that is responsible for cellular passive stiffness may contribute to high cardiomyocyte resting tension and thereby diastolic dysfunction in mRen2 rats.

We observed an increase in Ca^{2+}-independent (passive) tension, but no significant changes in Ca^{2+}-activated (active) force generation of left ventricular cardiomyocytes of mRen2 rats. Our mechanical experiments were performed on isolated skinned cardiomyocytes addressing intracellular factors selectively and independently of extracellular matrix for the first time. Indeed, reports on small cardiac biopsies from heart failure patients demonstrated that cardiomyocyte passive tension is increased in HFpEF, and that passive tension is being higher as compared to HFrEF. Accordingly, high cardiomyocyte resting tension is considered as the cellular trademark of diastolic dysfunction seen in HFpEF.

The main intracellular determinant of passive tension of the contractile machinery is the titin molecule, spanning the half sarcomere. Titin was directly studied in mRen2 rats here for the first time. Only the N2B titin isoform was expressed in the mRen2 heart without apparent signs of proteolytic degradation.

Intracellular angiotensin II activates PKCα-mediated protein phosphorylation, targeting titin in addition to other myofibrillar proteins. The expression level of PKCα was 1.8-fold increased in the left ventricle of mRen2 rats without change in the ratio of phosphorylated (Ser-657/Tyr-658) and total PKCα. These suggest elevated levels of activated (phosphorylated) PKCα in mRen2 rats.

We found no change in total titin phosphorylation as addressed by phospho-specific Pro-Q Diamond gel staining in mRen2 rats. Previous reports suggested that the PEVK domain cannot be detected by Pro-Q Diamond stain. However, PKCα phosphorylates titin's PEVK spring element at Ser-12742 and Ser-12884, apparently modulating cardiomyocyte titin-based stiffness. Accordingly, the PEVK phosphorylation was tested here with phospho-specific antibodies against phosphorylated Ser-12742 and Ser-12884 residues. We found increased phosphorylation of titin at Ser-12742, without changes in the phosphorylation level at Ser-12884 in the left ventricle mRen2 hearts. PEVK Ser-12742 hyperphosphorylation was

previously demonstrated in mice with transverse aortic constriction, in an old hypertensive dog model, as well as in human HFpEF associated with hypertension. Data suggest that a significant rise in collagen- and titin-dependent stiffness is paralleled by explicit changes in titin phosphorylation levels, e.g. PKCα-dependent hyperphosphorylation at Ser-11878 (Ser-12742 in the rat) of the PEVK element.

5.3. Original observations of the doctoral thesis

Based on the results of the doctoral thesis the following original statements are made:

- In hearts exposed to Ca^{2+} paradox degradation of α-MHC and cTnT is accompanied by altered myofibrillar ATPase activities and depressed Ca^{2+}-activated force generation of isolated cardiomyocytes, collectively contributing to impaired global pump function.

- In the transgenic mRen2 rat model of hypertension reduced myocardial ACE2 activity is accompanied by the PKCα-mediated hyperphosphorylation of the PEVK element (at Ser-12742) of titin, contributing to high cardiomyocyte passive tension.

6. SUMMARY

Isolated rat hearts suffered Ca^{2+} paradox demonstrate impaired global and cellular contractility that is accompanied by decreased Ca^{2+}-stimulated ATPase activity potentially as a result of myofilament protein degradation. According to data provided in this thesis, we conclude that significant deterioration in cardiac relaxation seen in Ca^{2+} paradoxical hearts is probably due to a failure in cross-bridge cycling because of an altered myofibrillar ATPase activity, and is apparently not related directly to titin. On the other hand, it is likely that one of the molecular bases of dramatic decrease in systolic function in Ca^{2+} paradox may be α-MHC and cTnT cleavage, resulting in a collective reduction of interdependent parameters of Ca^{2+}-activated force generation at the level of cardiomyocytes, myofibrils and isolated heart.

In hypertension due to the genetic stimulation of RAS signaling cellular and molecular basis of the left ventricular diastolic dysfunction correlates with the mechanistic changes seen in human HFpEF. Our results implicate the pathophysiological role of the imbalance of myocardial RAS pathways in the development of diastolic dysfunction. Data provided here suggest that hyperphosphorylation at Ser-12742 in the PEVK element of titin and increased cardiomyocyte passive tension are common features of diastolic dysfunction in RAS-mediated experimental hypertension and clinical HFpEF.

7. LIST OF PUBLICATIONS

UNIVERSITY OF DEBRECEN
UNIVERSITY AND NATIONAL LIBRARY

Registry number: DEENK/175/2017.PL
Subject: PhD Publikációs Lista

Candidate: Árpád Kovács
Neptun ID: K5539B
Doctoral School: Kálmán Laki Doctoral School

List of publications related to the dissertation

1. **Kovács, Á.**, Kalász, J., Pásztorné Tóth, E., Tóth, A., Papp, Z., Dhalla, N. S., Barta, J.: Myosin heavy chain and cardiac troponin T damage is associated with impaired myofibrillar ATPase activity contributing to sarcomeric dysfunction in Ca2+-paradox rat hearts.
   Mol. Cell. Biochem. 403 (1-2), 57-68, 2017.
   DOI: http://dx.doi.org/10.1007/s11010-017-2954-8
   IF: 2.613 (2015)
2. **Kovács, Á.**, Fülöp, G. Á., Kovács, A., Csípő, T., Bódi, B., Priksz, D., Juhász, B., Beke, L., Hendrik, Z., Méhes, G., Granzier, H. L., Édes, I., Fagyas, M., Papp, Z., Barta, J., Tóth, A.: Renin overexpression leads to increased titin-based stiffness contributing to diastolic dysfunction in hypertensive mRen2 rats.
   Am. J. Physiol.-Heart Circul. Physiol. 310 (11), H1671-H1682, 2016.
   DOI: http://dx.doi.org/10.1152/ajpheart.00842.2015
   IF: 3.324 (2015)

List of other publications

3. Nagy, L., Gödény, I., Nánási, P. P., Leskó, Á., Balogh, L., Bánhegyi, V., Bódi, B., Csípő, T., Csongrádi, A., Fülöp, G. Á., **Kovács, Á.**, Lódi, M., Papp, Z.: A szív pozitív inotróp támogatása a miozin-aktivátor hatású omecamtiv-mecarbil segítségével.
   Cardiol. Hung. 47 (1), 69-76, 2017.
4. **Kovács, Á.**, Alogna, A., Post, H., Hamdani, N.: Is enhancing cGMP-PKG signalling a promising therapeutic target for heart failure with preserved ejection fraction?
   Neth. Heart. J. 24 (4), 268-274, 2016.
   DOI: http://dx.doi.org/10.1007/s12471-016-0814-x
   IF: 2.062 (2015)

Address: 1 Egyetem tér, Debrecen 4032, Hungary Postal address: Pf. 39. Debrecen 4010, Hungary
Tel.: +36 52 410 443 Fax: +36 52 512 900/63847 E-mail: publikaciok@lib.unideb.hu, ¤ Web: www.lib.unideb.hu

5. Barta, J., **Kovács, Á.**: Szívelégtelenség és cilostazol.
Cardiol. Hung. 45 (2), 108-116, 2015.

6. Nagy, L., **Kovács, Á.**, Bódi, B., Pásztorné Tóth, E., Fülöp, G. Á., Tóth, A., Édes, I., Papp, Z.: The novel cardiac myosin activator omecamtiv mecarbil increases the calcium sensitivity of force production in isolated cardiomyocytes and skeletal muscle fibres of the rat.
Br. J. Pharmacol. 172 (18), 4506-4518, 2015.
DOI: http://dx.doi.org/10.1111/bph.13235
IF: 5.259

7. **Kovács, Á.**, Papp, Z., Nagy, L.: Causes and pathophysiology of heart failure with preserved ejection fraction.
Heart Fail. Clin. 10 (3), 389-398, 2014.
DOI: http://dx.doi.org/10.1016/j.hfc.2014.04.002
IF: 1.844

8. Balogh, Á., Tóth, A., Pásztorné Tóth, E., Nagy, L., **Kovács, Á.**, Kalász, J., Contreras, G. A., Édes, I., Papp, Z.: Myofilament carbonylation modulates contractility in human cardiomyocytes.
Exp. Clin. Cardiol. 20 (1), 2026-2035, 2014.

Total IF of journals (all publications): 15,102
Total IF of journals (publications related to the dissertation): 5,937

The Candidate's publication data submitted to the iDEa Tudóstér have been validated by DEENK on the basis of Web of Science, Scopus and Journal Citation Report (Impact Factor) databases.

14 June, 2017

DEBRECENI EGYETEM KENÉZY ÉLETTUDOMÁNYI KÖNYVTÁRA EGYETEMI ÉS NEMZETI KÖNYVTÁR

8. ACKNOWLEDGEMENT

Firstly, I would like to express my sincere gratitude to my supervisor *Judit Barta*, whose exceptional accuracy and professionalism served me as a top standard during my PhD. I am very grateful for supporting me as a PhD student to reach my goals. I hope that our work does not come to an end after receiving my PhD degree.

It has been a real pleasure and a learning experience to work with all my mentors during my PhD at my home university. I would like to express my appreciation to *professor Zoltán Papp*, the Head of the Division of Clinical Physiology, for the help and support in my scientific career. I thank to *professor Attila Tóth* for performing our experiments together. It has been a great pleasure to work with him. I am very grateful to *professor István Édes*, the Head of the Department of Cardiology, for his continuous help and support in my career.

My sincere also goes to *Ágnes Balogh, Dániel Czuriga and Gábor Áron Fülöp* for their honest and friendly support. Their standards and atmosphere at work guide me day by day. In addition, my thanks are extended to all the previous and present co-workers at the Division of Clinical Physiology for their plenty of help and time during my PhD.

I thank to my Wife and Family for their continuous faith and support.

The doctoral thesis is supported by the GINOP-2.3.2-15-2016-00043. project. The project is co-financed by the European Union and the European Regional Development Fund. SUPPORTED THROUGH THE NEW NATIONAL EXCELLENCE PROGRAM OF THE MINISTRY OF HUMAN CAPACITIES.